Application of Liquid Metal Antenna in Bridges as a Strain Sensor

Edmon O. Fernandez#1, Lejan Alfred C. Enriquez#2 Arielle Jan L. Bautista#3, Alyssa Celine C. Castillo#4, Justine Gerald V. Saavedra#5, Trisha M. Salanatin#6, Toni Rose M. Soriano#7

Electronics Engineering Department, Technological University of the Philippines

Manila, Philippines

[1]edmon_fernandez@tup.edu.ph

[2]lejanalfred_enriquez@tup.edu.ph

[3]ariellejan.bautista@tup.edu.ph

[4]alyssaceline.castillo@tup.edu.ph

[5]justinegerald.saavedra@tup.edu.ph

[6]trisha.salanatin@tup.edu.ph

[7]tonirose.soriano@tup.edu.ph

***Abstract* – This study develops a Structural Health Monitoring System that will track the strain imbued within the concrete. This system is composed of a liquid metal antenna, sensing unit, microcontroller, and computer application. The resonant frequency is the main input of this study that changes as the liquid metal antenna stretches or contracts. This resonant frequency is converted into voltage readings by the sensing unit. A Wireless Sensor Network is to accompany the microcontroller that will read and save the voltage readings of the sensing unit. This network is a star topology network that uses Zigbee Technology for data acquisition. A computer application is also developed to generate reports of the strain detected by the sensors, displaying the short- and long-term predictions, plotting the data, and sensor settings to specify which data to show. To test the validity of the system, the resonant frequency of the liquid metal antenna acquired by the NanoVNA is compared to the data gathered by the system.**

Experiments showed that there is a direct relationship between the voltage and the resonant frequency of the LMA in the system, as the resonant frequency decreases the voltage decreases. Hence, there is an inverse relationship between voltage and strain applied, as the LMA resonance frequency decreases due to the increasing strain imbued resulting in its elongation, the voltage decreases as well.

***Keywords* – liquid metal antenna, resonant frequency, harmonic termination network, wireless sensor network, Zigbee protocol, sensor node**

I. INTRODUCTION

Important structures such as roads and bridges are susceptible to wear and tear from regular usage by vehicles which can vary from light motorcycles to heavy-duty transportation trucks. These loads induce strain on the surfaces of the roads and bridges thus causing strain. Since the country is in the Pacific Ring of Fire, it is important that the Philippines must have excellent Structural Health Monitoring. The Structural Health Monitoring (SHM) done in the Philippines was based only on the physicality of the structures and can be considered inaccurate, which is the reason why buildings, roads, and bridges are still at risk whenever disasters occur. Technology advancements in Structural Health Monitoring include strain gauges, sensor nodes, and automated monitoring [7].

A promising technology as a viable replacement for strain gauges is Liquid Metal Antenna (LMA). These can be applied in SHM due to their size, light-weightiness, non-complex design, flexibility, and self-healing properties. Strain can be detected by its resonant frequency being inversely proportional to its displacement [3]. To implement LMA into the proposed SHM system, a sensing unit would be designed and constructed. The sensing unit would read the resonant frequency of LMA when strain is applied to the reinforced concrete and convert them to voltage, then pass through an Arduino Uno where the signal undergoes analog-to-digital conversion.

The SHM system in this project study utilized the use of wireless communication to connect all components: LMAs, sensing units, WSN devices, and a computer application. The system shall be composed of sensor nodes, where each sensing unit was connected to the Arduino Uno and Zigbee wireless module to recognize data acquired from LMA, and a single master node with a USB communication interface for transferring data to the computer application of SHM system.

IEEE 802.15.4 standard implemented Zigbee that specifies high-level communication protocol mainly used for wireless data transmission up to 100 meters at a fixed speed of 250 kbps [8]. Using this protocol, wireless SHM will be obtained, and the strain in specific points can be detected by the multiple nodes of the strain sensor which provide better accuracy of readings.

The elements used for analyses are based on the experimental setups for Liquid Metal Antenna equipping NanoVNA and the sensing unit as a tool for acquiring data. It is crucial for this study to compare the results of two different tools, NanoVNA and Sensing Unit because it strengthens the validity and precision of the developed Structural Health Monitoring System.

II. METHODOLOGY

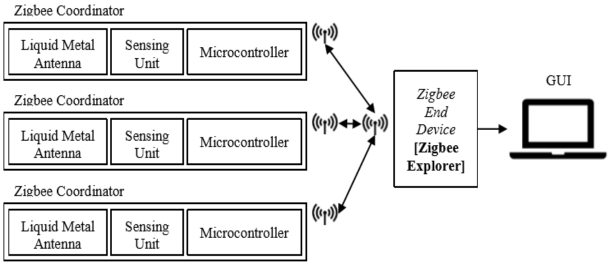

Figure 1. System Architecture

The overall system of this study is shown in Figure 1. It consists of wired and wireless connections between devices from the input to the output. The system consists of three major parts: input system, data processing, and output system. The system starts with equipping the liquid metal antenna as a strain sensor which acquires their respective resonant frequency. Then, the circuits of sensing units are designed to obtain the input from liquid metal antenna and convert it to voltage pulses and these are connected to Arduino UNO. The location of sensing units and Arduino UNO modules are on the structure side and considered the sensor node of the network. The relevant information acquired is sent to the master node operated by the system unit, through wireless communication using Zigbee end-device and Zigbee coordinators.

Each Arduino UNO for the sensor nodes has a storage device module for saving data when the sensors are not actively connected to the master node. The master node consists of a Zigbee module with Zigbee explorer connected directly to the system unit for graphical user interface (GUI) which is located at the end-user side. Lastly, the Structural Health Monitoring System computer application shows the integrity of the structure in terms of strain with diagrams, warnings, and predictions.

A. Liquid Metal Antenna

This device is designed to act as a strain sensor for the SHM system and it is fabricated using Soft Lithography. Eutectic Gallium Indium is the liquid metal used and the substrate is the QSIL 216 which is a type of polydimethylsiloxane. An adhesive is used to attach the liquid metal antenna and the sensing unit under the bridge. The adhesive used is the El Heneral all-purpose epoxy because it exhibits strong adhesion in all types of weather.


Figure 2. Liquid Metal Antenna and Sensing Unit attached under the bridge

B. Sensing Unit Architecture

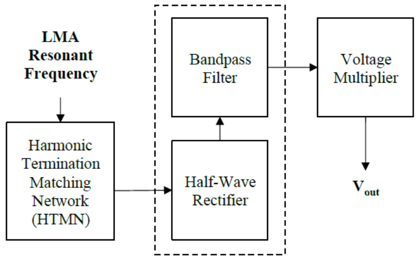

Figure 1. Sensing Unit Block Diagram

The Sensing Unit design was based on the design made by Au & Seo [10] and Schauwecker [1]. The circuit starts off with the Harmonic Termination Matching Network (HTMN), which had two purposes: 1) impedance matching and 2) harmonic suppression. This part of the circuit was based on the stub matching concept for transmission lines and microstrip filters. To construct the HTMN, the proponents used Keysight Advanced Design System software for its Line Calculation Feature which helped in getting the dimensions of HTMN.

C. Wireless Sensor Network

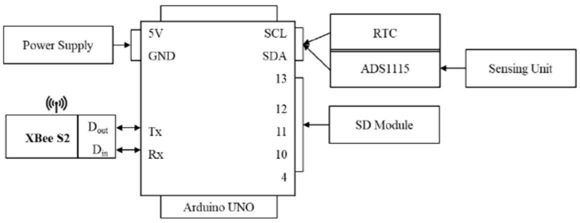

Figure 3. Sensor Node for Wireless Communications System

The sensor nodes consisted of the sensing unit connection, Arduino Uno, Zigbee wireless modules, SD card module, Real-time clock module, ADC Bit converter, and power supply are responsible for acquiring data from the sensing unit and sending measured values to the master node.

The microcontroller utilized for sensor nodes was the Arduino Uno module with ATMEGA328P and its main purpose was to acquire voltage pulses from the sensing unit and process data that would be prepared for delivering to the Zigbee wireless module. ADS1115 is utilized to have higher resolution output data with 16-bit ADC, which has an adjustable gain allowing it focus within millivolt to microvolt range in 16-bit resolution. XBee Shield was used for seamless interface between the Arduino module and the XBee S2. It can also store data in the micro-SD card and to have reliable time indication of data acquired, RTC module DS3231 was used to record the time occurrence of data. The power supply used was a Lithium Polymer (Li-Po) battery which was rechargeable connected to the 5V pin of the Arduino module.

Figure 4. Wireless Sensor Network device installed on the bridge

The master node consisted of an XBee Explorer module with XBee S2 Mesh C module connected via USB communication interface to the system unit is responsible for wirelessly receiving data from the sensor nodes and transporting measured values to the system unit for GUI and its base module is FTDI device which aims to have a simple transceiver device to recognize data received by the XBee S2 and send commands to the sensor nodes.

D. Computer Application

In this study, a python-based computer program aided with API libraries such as PyQT5 for the GUI building aspect and, pySerial and Arduino's Firmata for the serial port connection and communication between the computer and Arduino. PyQT5 is a GUI (Graphical User Interface) that is more versatile than the de-facto standard Tkinter. pySerial is a module that encapsulates the access for the serial port [5]. Firmata is a communications protocol fully implemented on Arduino for communicating between the microcontroller and the computer [2]. The features included in the computer application are:

1. Sensors Report which is comprised of the short- long-term reports. It also includes prediction reports that use Regression analysis to predict the trend of the sensor's reading.
2. Dynamic Graph (Live-view/Free-view) for plotting a set range of data gathered by the GUI. When in real-time mode, it will automatically plot and update each new data instance.
3. Sensor settings are also included to give space for customization of threshold appropriate for its placement on the structure. Here, you can also add and remove sensors when needed along with the configurations in the Zigbee connection.

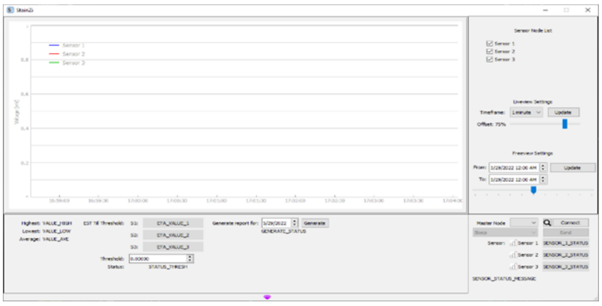

Figure 5. Graphic User Interface of the System Prototype Computer Application

Figure 6 shows the workflow of the GUI computer application. The GUI did not require a connection to the master node beforehand to run. Connecting to the master node enables to send three specific commands: 'put the WSN to sleep', initiate real-time mode', and 'initiate user-time mode'. The two latter enables the GUI to receive the data from the WSN and save them on a CSV file depending on their indicated date. If the WSN was set to real-time mode, then the received data will also be plotted on the GUI graph. Settings for both live-view and free-view settings are at the side of the GUI window which affects how the graph will update. Toggled visible sensors also affect the plotting from this mode. The GUI graph, once given an update to its graph, would calculate the trendline and general statistics of its plot data and update the sensor report. Lastly is the Generate Report which would generate the report for a given day. It does calculations similar to the GUI graph and generates a PDF file containing the plot and calculations from the data of the given date.

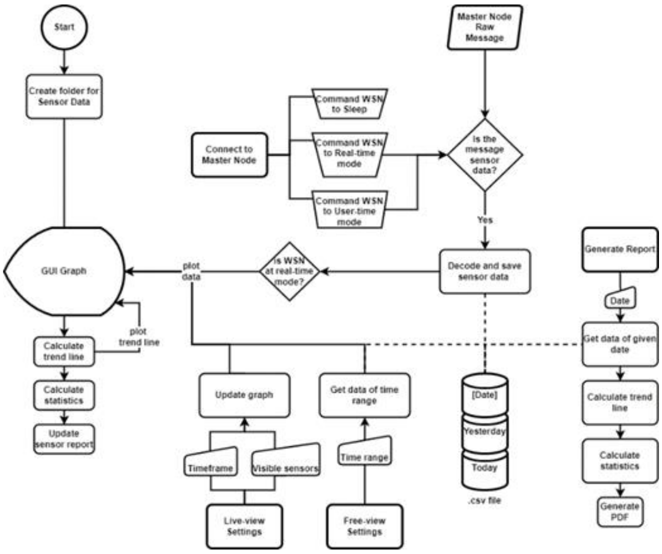

Figure 6: Program Workflow for Computer Application GUI

E. Deployment Setup

For the deployment plan, the proponents need to ask for permission and assistance from the Department of Public Works and Highways (DPWH) – Pampanga, Candaba LGU, and San Agustin Barangay Office to deploy their study on San Agustin "Bomba" Bridge. Assistance from Civil Engineers was needed on to where the LMA should be attached. The proponents would need to follow the health protocol of their deployment location.

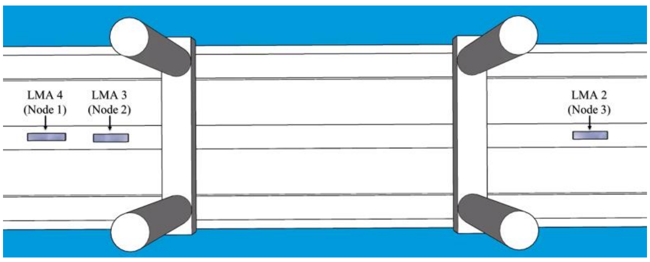

Figure 7: Liquid Metal Antenna Deployment Setup

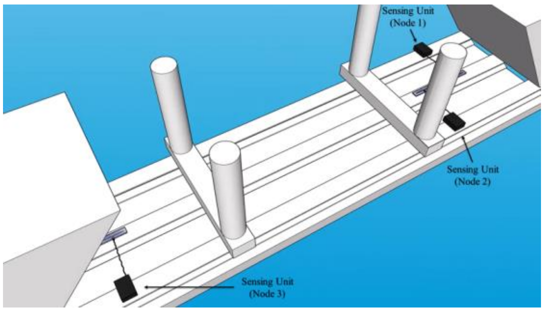

Figure 8. Sensing Unit Deployment Setup

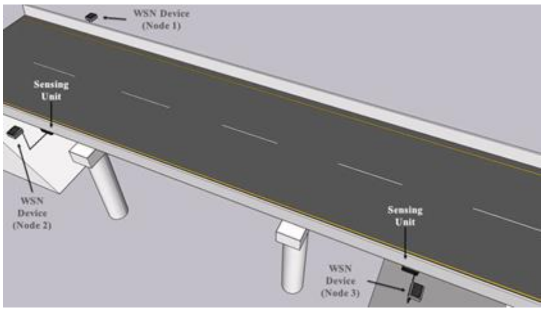

Figure 9. WSN Device Deployment Setup

F. Testing Procedures

The data gathered by the proponents of the project study would be subjected to statistical treatment. For each sensor nodes, the proponents gathered data before, during, and after a vehicle passed the bridge. These voltage data were subtracted to get the data prior (during - before) and subsequent (after – during) to passing the bridge. these data instances would be classified per vehicle class as per the vehicle classification released by the Department of Transportation [13]. Since there would be plenty of data that would be recorded, the proponents would get the average of each vehicle class for more clearer visualization of data. Once such graphs were obtained per sensor node, the average, data prior, and subsequent would be plotted altogether.

III. Results And Discussion

The data analysis and results were categorized and presented in four sections: 1) Data Collection 2) Simulation Data 3) Actual Data and 4) Data Results from Computer Application. The data were collected and interpreted in response to the objective that is mentioned in Chapter 1. The objectives were to develop the feasibility of the Liquid Metal Antenna as a sensor in Structural Health Monitoring. This also included the justification of data in case no statistical results were found.

A. Data Collection

Based on the journal article in [12], the average weight of a tricycle is 201 kg, whereas the motorcycle weighs 75 kilograms. The L300 used for commercial purposes has a weight of 2345 according to the specifications given by Zigwheels. Moreover, in a separate article by Nealon, she listed down different types of cars and their corresponding weight. The car weighs 680 to 1995 kilograms and this ranges from smart cars, compact cars, and midsize cars to large cars. The SUV weighs 907 to 2721 kilograms and this ranges from compact SUVs to midsize SUVs to large SUVs. On the other hand, the pick-up truck (half-ton truck) weighs 2449 to 2494 kilograms. The weights of different types of trucks when loaded are also included, whereas the food truck weighs up to 35153 kilograms (40 tons), the dump truck weighs up to 32659 kilograms (36 tons) and the fire truck weighs up to 17237 to 27216 kilograms (19 to 30 tons).

Table 1. Weight of Vehicles by Type and Class

Vehicle Category	Type of Vehicle	Weight (kg)
Class 1-A	Motorcycle	75
	Tricycle	200
Class 1-B	Car	700 – 2000
	SUV	900 – 2700
	Pick-up	2500
	L300	2350
Class 2	Trucks	6100
Class 3	Food Truck (loaded)	35000
	Dump Truck (loaded)	33000
	Fire Truck (loaded)	17000 – 27000

To determine the possible threshold that the Liquid Metal Antenna can be stretched before it can reach its limit and to determine the minimum possible resonant frequency the Liquid Metal Antenna can produce. This will serve as the basis for the values of resonant frequency that the Liquid Metal Antenna would acquire during the actual deployment. From Table 2, depending on the sensitivity of the LMA, its resonant frequency can decrease by 35 MHz to 153 MHz.

Table 2. The threshold of LMA when stretched

LMA	Resonant Frequency at Rest	Resonant Frequency at Threshold	Threshold Stretch (per mm)	LMA Status
01	702 MHz	666 MHz	145 - 165	Active
02	783 MHz	648 MHz	145 – 165	Active
03	738 MHz	585 MHz	145 - 165	Damaged

B. Simulated Data

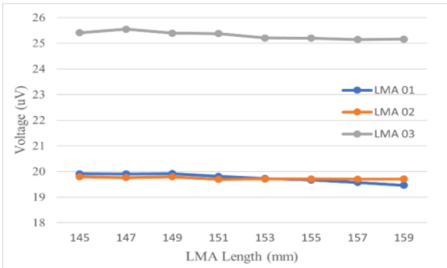

Figure 10. Graph of Voltage acquired by the Sensing Unit vs. LMA Length

From the data gathered and the graph shown in Figure 11, as the Liquid Metal Antenna elongates, the average output voltage read by the system decreases. Therefore, since the resonant frequency decreases as the antenna elongates, and the average output voltage read by the system also decreases, there is a direct relationship between the antenna's resonant frequency and output voltage. When strain is applied to the antenna, it is expected that there will be a decrease in output voltage that will be read by the system.

C. Actual Data

The graph shows the average output voltage of all vehicles in each category of vehicle gathered from Sensor Node 1, Sensor Node 2, and Sensor Node 3. From the gathered data, the higher the class or the heavier the vehicle which passes by the bridge, the larger average output voltage difference is read by the system.

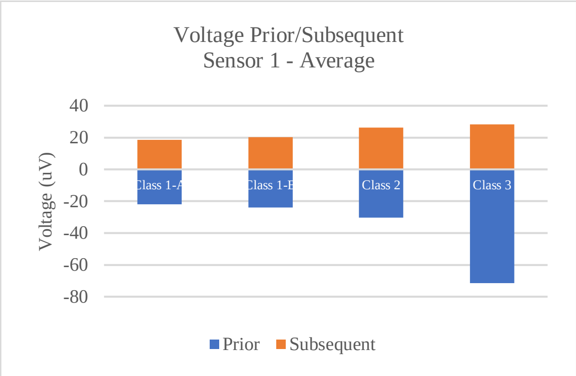

Figure 11. Average Voltage Difference for Sensor Node 1

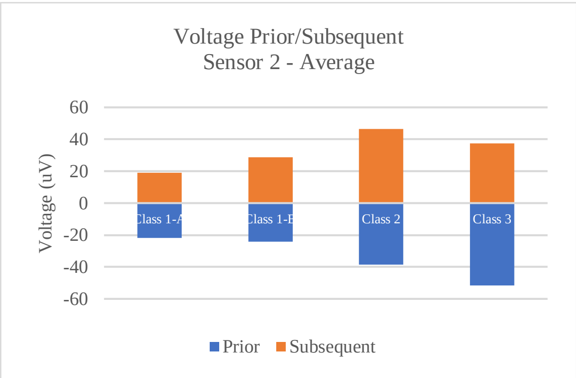

Figure 12. Average Voltage Difference for Sensor Node 2

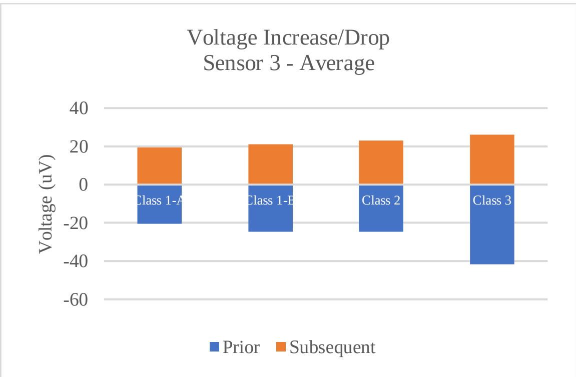

Figure 13. Average Voltage Difference for Sensor Node 3

The following graph shows the instances recorded from all the sensor nodes under Class 1-A, Class 1-B, Class 2, and Class 3. The Prior and Subsequent data show the before and after of passing of the vehicle from the bridge respectively. There reflects the data between prior and subsequent which correlates to the output voltage when a vehicle passes through the bridge detected by the system. There is no significant difference between the voltage output of vehicles under this class.

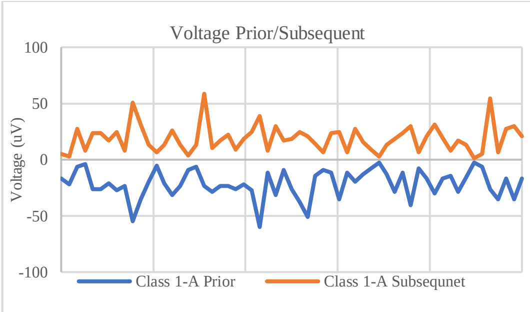

Figure 14. Voltage Difference per Vehicle under Class 1-A

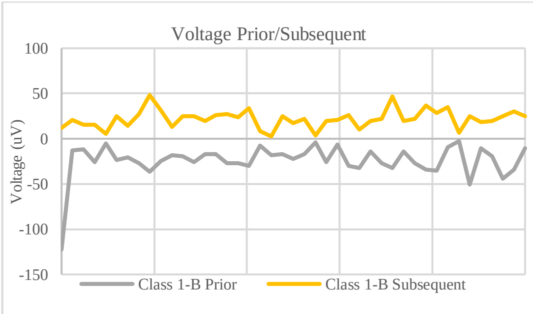

Figure 15. Voltage Difference per Vehicle under Class 1-B

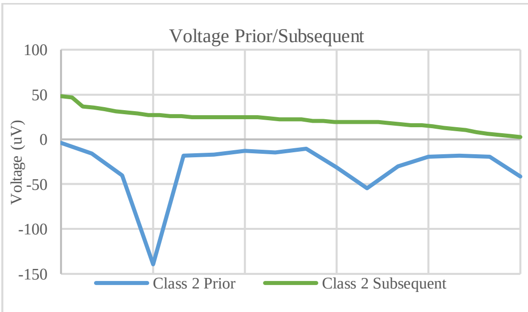

Figure 16. Voltage Difference per Vehicle under Class 2

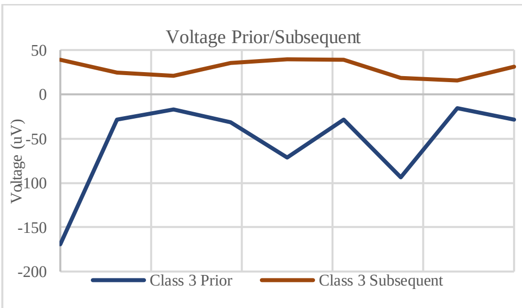

Figure 17. Voltage Difference per Vehicle under Class 3

D. Data Results from Computer Application

Figure 18 shows the data gathered of the system using the STRAINZI computer application from the deployment in the actual bridge. Based on the confirmation of the end-user between real-time and user-time operation, the history of data saved in the computer is shown by adjusting the date and time of the map diagram. The blue line indicates sensor node 1, the red line for sensor node 2, and the green line for sensor node 3. As shown in the map diagram, the voltage decreases at certain times indicating a vehicle arrived at the bridge.

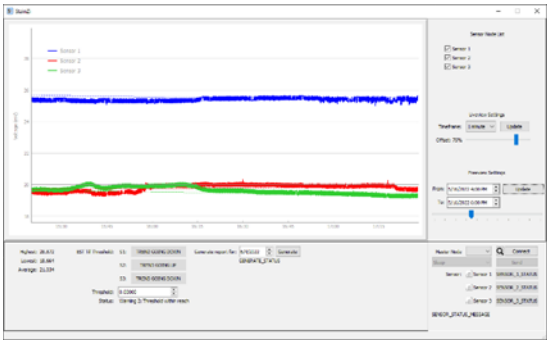

Figure 18. System Prototype Computer Application containing the data from the bridge deployment

IV. Conclusion

Based on the findings and results of the study, the following were the conclusions drawn:

1. The designed and fabricated twenty-to Liquid Metal Antennas using Eutectic Gallium Indium (EGaIn) liquid metal and Polydimethylsiloxane (PDMS) substrate via Soft Lithography were measured theoretically of 603.5 MHz resonant frequency that varies output on external factors, and length of 145 mm at rest to 159 mm at 14 mm maximum stretch.
2. The established Wireless Sensor Network (WSN) with star topology was composed of four transceivers having a single master node and three sensor nodes with the real-time and user-time operation that used 16-bit ADC module ADS1115 to recognize the small range of data from the sensing units and operated with solar panels
3. The developed computer application generated diagrams of voltage data acquired from the sensor nodes with short- to long-term predictions of data using linear regression embedded on the application, implemented warning through threshold status of data, and report generation in Portable Document Format (PDF).
4. The results gathered from the study showing the prior and subsequent voltage data corresponding respectively to begore and after the passing of the vehicle from the bridge was assessed and validated by the civil engineers employed in DPWH-Pampanga First District Engineering Office Design and Planning Section.

V. Recommendations

To further improve the study, future researchers may consider developing and designing a Sensing Unit circuit that would yield DC Voltage rather than Voltage pulses for easier data readings. It is also advisable to use other wireless mediums that allow all sensors to be in range at any point on the bridge to allow for a reliable uninterrupted connection. Lastly, it is also recommendable to find a better adhesive that would not affect the Liquide Metal Antenna's sensitivity in sensing strain in concrete beams. For the deployment, it is better if there would be more disciplines involved such as electrical engineering, mechanical engineering, and civil engineering. The electrical wirings in the deployment must also be more secured and it is recommended to use a conduit system for it.

Acknowledgement

This study is made possible with the guidance of Engr. Edmon O. Fernandez and Engr. Lejan Alfred C. Enriquez, the advisers of this study, together with the panel members, Engr. Juan Paulo L. Bersamina, Engr. John Peter M. Ramos, Engr. Gilfred Allen M. Madrigal, Engr. Romeo L. Jorda Jr., Engr. Edmund G. Monilar, and Engr. Cherry G. Pascion who gives an intuitive opinion, omnific suggestions, and rational criticism for the betterment of the study. Researchers also would like to thank the DOST Electronic Product Development Center for fabricating the designed sensing unit, and the Planning and Design Section of the First District Engineering Office of DPWH Pampanga for aiding in the deployment of this study. Engr. Jefferson M. Soriano for designing and producing the bracket mount of Wireless Sensor Network, Jade Meler Senosa, for giving assistance in procurement of materials, Bautista, and Soriano family for providing the team a comfortable stay in their homes, to the families of the team for the support and unconditional love that inspires them to complete it. Lastly, to God Almighty who gives them strength, wisdom, and skill all throughout this study.

References

[1] B. Schauwecker, *Design of Processing Circuitry for an RF energy Harvester*, Undergraduate Thesis, University of Arkansas, Fayetteville, 2016. [Online]. Available: https://scholarworks.uark.edu/eleguht/48/

[2] DPWH, (2019, Mar. 25). BOD SET No. 2018-5 BrD, *STANDARD MULTI SPAN REINFORCED CONCRETE DECK GIRDER (RCDG) BRIDGES*, [Online]. Available: https://www.dpwh.gov.ph/dpwh/sites/default/files/references/standard_design/Standard%20Plan%20for%20%20Multi%20Span%20RCDG%20Bridge.pdf

[3] E. Fernandez, A. Carandang, J.W. Orillo, L.R. Quezada, I. Valenzuela, and V. Yee, *Determination of Optimum Placement of the Liquid Metal Antenna Design Embedded in Concrete Beam Prototype Under Center – Point Loading Test*, in 7th IEEE International Conference Humanoid, Nanotechnology, Information Technology, Communication and Control, Environment and Management (HNICEM), Philippines 2013.

[4] G. Chaudhary, P. Kim, Y.C. Jeong, and J.H. Yoon, *Design of a High Efficiency RF-DC Conversion Circuit using Novel Termination Networks*

for RF Energy Harvesting System, Microwave and Optical Technology Letters, volume 54 no. 10, pp. 2330 – 2335, 2012.

[5] Github, [Online]. Available: https://github.com/pyserial/pyserial/

[6] H.C. Steiner, *Firmata: Towards Making Microcontrollers Act Like Extensions of the Computer*, NIME, volume 9, pp. 125 – 130, 2009.

[7] J. dos Reis, C. Oliveira Costa, and J. Sá da Costa, *Strain gauges debonding fault detection for structural health monitoring*, Structural Control and Health Monitoring, vol. 25, no. 12, Sep. 2018, DOI: 10.1002/stc.2264.

[8] Kumar and S. Bhatia, *ATMega 328 Based Menu Ordering System Using Zigbee*, International Journal of Scientific & Technology Research, Volume 4 Issue 6, pp. 124-125, 2015.

[9] M. Kubo, X. Li, C. Kim, M. Hashimoto, B. J. Wiley, D. Ham, and G. M. Whitesides, *Stretchable microfluidic radiofrequency antennas*, Advanced Materials, vol. 22, no. 25, pp. 2749–2752, 2010.

[10] N. D. Au and C. Seo, *A Novel Design of an RF-DC Converter for a Low–Input Power Receiver*, Journal of Electromagnetic Engineering and Science, vol. 17, no. 4, pp. 191–196, Oct. 2017, DOI: 10.26866/jees.2017.17.4.191.

[11] R. Govindarajan, S. Meikandasivam, and D. Vijayakumar, *Energy Monitoring System Using Zigbee and Arduino*, International Journal of Engineering & Technology, volume 7 no. 4.28, pp. 608 – 611, 2018. XBEE2, XBEEPRO2

[12] [63] J. B. M. Biona, A. B. Culaba, and M. R. I. Purvis, *Energy Use and Emissions of Two stroke-powered Tricycles in Metro Manila*, Transportation Research Part D: Transport and Environment, vol. 12, no. 7, pp. 488–497, Oct. 2007, DOI: 10.1016/j.trd.2007.06.005.

[13] [60] Toll Regulatory Board, *Vehicle Classifications.* Accessed: May 30, 2022. [Online]. Available: https://trb.gov.ph/index.php/faqs/vehicle-classification